

Blood-derived mitochondrial DNA copy number is associated with gene expression across multiple tissues and is predictive for incident neurodegenerative disease

— [Source link](#) 

Stephanie Y. Yang, Christina A. Castellani, Ryan J. Longchamps, Vamsee Pillalamarri ...+3 more authors

Institutions: Johns Hopkins University School of Medicine, Johns Hopkins University

Published on: 18 Jul 2020 - bioRxiv (Cold Spring Harbor Laboratory)

Topics: Mitochondrial DNA replication, Gene expression, Gene, NRF1 and Whole blood

Related papers:

- [Blood-derived mitochondrial DNA copy number is associated with gene expression across multiple tissues and is predictive for incident neurodegenerative disease.](#)
- [Mitochondrial DNA Copy Number \(mtDNA-CN\) Can Influence Mortality and Cardiovascular Disease via Methylation of Nuclear DNA CpGs](#)
- [Mitochondrial DNA copy number can influence mortality and cardiovascular disease via methylation of nuclear DNA CpGs.](#)
- [Genetic analysis of mitochondrial DNA copy number and associated traits identifies loci implicated in nucleotide metabolism, platelet activation, and megakaryocyte proliferation, and reveals a causal association of mitochondrial function with mortality](#)
- [Genome-wide mitochondrial DNA sequence variations and lower expression of OXPHOS genes predict mitochondrial dysfunction in oral cancer tissue.](#)

Share this paper:    

View more about this paper here: <https://typeset.io/papers/blood-derived-mitochondrial-dna-copy-number-is-associated-2fmep2ca4q>

1 **Blood-derived mitochondrial DNA copy number is associated with gene expression across multiple**
2 **tissues and is predictive for incident neurodegenerative disease**

3
4 Stephanie Y. Yang¹, Christina A. Castellani¹, Ryan J. Longchamps¹, Vamsee K. Pillalamarri¹, Brian
5 O'Rourke², Eliseo Guallar³, Dan E. Arking^{1,2}
6

7
8 ¹McKusick-Nathans Department of Genetic Medicine, Johns Hopkins University School of Medicine,
9 Baltimore, MD

10 ²Division of Cardiology, Department of Medicine, Johns Hopkins University School of Medicine,
11 Baltimore, MD

12 ³Departments of Epidemiology and Medicine, and Welch Center for Prevention, Epidemiology, and
13 Clinical Research, Johns Hopkins University Bloomberg School of Public Health, Baltimore, MD
14

15 **Email addresses:**

16 syang93@jhmi.edu

17 ccastell8@jhmi.edu

18 rlongcha@broadinstitute.org

19 vpillal1@jhmi.edu

20 bor@jhmi.edu

21 eguallar@jhmi.edu

22 arking@jhmi.edu
23

24

25

26

27

28

29

30

31

32

33

34

35 *Correspondence and address for reprints to:

36 Dan E. Arking, Ph.D.

37 Johns Hopkins University School of Medicine

38 733 N Broadway Ave

39 Miller Research Building Room 459

40 Baltimore, MD 21205

41 (410) 502-4867 (ph)

42 arking@jhmi.edu

43 **ABSTRACT**

44 ***Background***

45
46 Mitochondrial DNA copy number (mtDNA-CN) can be used as a proxy for mitochondrial function and is
47 associated with a number of aging-related diseases. However, it is unclear how mtDNA-CN measured in
48 blood can reflect risk for diseases that primarily manifest in other tissues. Using the Genotype-Tissue
49 Expression Project, we interrogated the relationships between mtDNA-CN measured in whole blood and
50 gene expression from whole blood as well as 47 additional tissues.

51 ***Results***

52 We evaluated associations between blood-derived mtDNA-CN and gene expression in whole blood for
53 418 individuals, correcting for known confounders and surrogate variables derived from RNA-
54 sequencing. Using a permutation-derived cutoff ($p < 2.70e-6$), mtDNA-CN was significantly associated
55 with expression for 721 genes in whole blood, including nuclear genes that are required for
56 mitochondrial DNA replication. Significantly enriched pathways included splicing ($p = 1.03e-8$) and
57 ubiquitin-mediated proteolysis ($p = 2.4e-10$). Genes with target sequences for the mitochondrial
58 transcription factor NRF1 were also enriched ($p = 1.76e-35$).

59 In non-blood tissues, there were more significantly associated genes than expected in 30 out of 47
60 tested tissues, suggesting that global gene expression in those tissues is correlated with mtDNA-CN.

61 Pathways that were associated in multiple tissues included RNA-binding, catalysis, and
62 neurodegenerative disease. We evaluated the association between mtDNA-CN and incident
63 neurodegenerative disease in an independent dataset, the UK Biobank, using a Cox proportional-hazards
64 model. Higher mtDNA-CN was significantly associated with lower risk for incident neurodegenerative
65 disease (HR=0.73, 95% CI= 0.66;0.90).

66 ***Conclusions***

67 The observation that mtDNA-CN measured in whole blood is associated with gene expression in other
68 tissues suggests that blood-derived mtDNA-CN can reflect metabolic health across multiple tissues. Key
69 pathways in maintaining cellular homeostasis, including splicing, RNA binding, and catalytic genes were
70 significantly associated with mtDNA-CN, reinforcing the importance of mitochondria in aging-related
71 disease. As a specific example, genes involved in neurodegenerative disease were significantly enriched
72 in multiple tissues. This finding, validated in a large independent cohort study showing an inverse
73 association between mtDNA-CN and neurodegenerative disease, solidifies the link between blood-
74 derived mtDNA-CN, altered gene expression in both blood and non-blood tissues, and aging-related
75 disease.

76

77

78

79

80

81

82

83

84

85

86

87 **BACKGROUND**

88 Mitochondria perform multiple essential metabolic functions including energy production, lipid
89 metabolism, and signaling for apoptosis. Mitochondria possess circular genomes (mtDNA) that are
90 distinct from the nuclear genome. While cells typically only possess two copies of the nuclear genome,
91 they contain 100s to 1000s of mitochondria, and each individual mitochondrion can hold 2-10 copies of
92 mtDNA resulting in wide variation in mtDNA copy number (mtDNA-CN) [1]. The amount of mtDNA-CN
93 also varies widely across cell types, with higher energy demand cell types typically possessing higher
94 levels of mtDNA-CN [1–3]. Due to the importance of mitochondria in metabolism and energy
95 production, mitochondrial dysfunction plays a role in the etiology of many human diseases [4]. mtDNA-
96 CN has been shown to be a proxy for mitochondrial function, and is consequently an attractive
97 biomarker due to its ease of measurement [5,6]. Indeed, low levels of mtDNA-CN in peripheral blood
98 have been associated with an increased risk for a number of chronic aging-related diseases including
99 frailty, kidney disease, cardiovascular disease, heart failure, and overall mortality [7–10].

100 Crosstalk between the mitochondrial and nuclear genomes is essential for maintaining cellular
101 homeostasis. Many essential mitochondrial proteins are encoded by the nuclear genome, and
102 expression of these nuclear genes must be modified to match mitochondrial activity. Likewise,
103 mitochondrial activity must respond to cellular energy demands. Polymorphisms in the nuclear genome
104 have been associated with changes in mitochondrial gene expression, and mitochondrial genome
105 variation has been associated with changes in nuclear gene expression, suggesting interplay between
106 the two genomes [11,12].

107 In cancer cells, mtDNA-CN alters gene expression through modifying DNA methylation [13,14]. Recent
108 work from our lab has shown that mtDNA-CN is also associated with nuclear DNA methylation in
109 noncancer settings [15]. Given that DNA methylation can modify gene expression, the current study
110 seeks to explore the potential association between blood-derived mtDNA-CN and gene expression. Past

111 work has shown that mtDNA-CN is associated with gene expression of nuclear-encoded genes in
112 lymphoblast cell lines, but this may not reflect biological processes occurring in other tissues, especially
113 after an extended culturing period [16]. Therefore, we leveraged data from the Genotype-Tissue
114 Expression Project (GTEx), a cross-sectional study with gene expression data from multiple non-diseased
115 postmortem tissues, to examine associations between mtDNA-CN and expression of both nuclear and
116 mitochondrially-encoded genes [17]. We found that blood-derived mtDNA-CN was globally associated
117 with increased gene expression in whole blood. Additionally, blood-derived mtDNA-CN was associated
118 with gene expression in other, non-blood tissues across the body. Specifically, genes annotated with
119 neurodegenerative disease pathways were significantly enriched, leading to a follow-up analysis that
120 uncovered a novel association between blood-derived mtDNA-CN and incident neurodegenerative
121 disease.

122

123 **RESULTS**

124 ***Determination and validation of mtDNA-CN metric***

125 mtDNA-CN estimates were generated from whole genome sequences performed on DNA derived from
126 whole blood using the ratio of mitochondrial reads to total aligned reads. As mtDNA-CN is known to be
127 affected by cell type composition, cell counts for samples with available RNA-sequencing data were
128 deconvoluted using gene expression measured in whole blood [18,19]. We identified a batch effect that
129 resulted in significantly altered mtDNA-CN for individuals sequenced prior to January 2013. Therefore,
130 only individuals sequenced after January 2013 were retained for analysis (Supp. Fig. 1). After quality
131 control, outlier filtering, and normalization of the RNA-sequencing data, 418 individuals remained for
132 analyses (see **Methods**).

133 To validate mtDNA-CN measurements in the filtered GTEx data, we determined the association between
134 mtDNA-CN and known correlated measures, including age, sex, and neutrophil count [18,20,21]. We

135 observed a significant association with neutrophil count ($p=5e-05$), with higher neutrophil count
136 associated with lower mtDNA-CN. While not statistically significant, effect size estimates between
137 mtDNA-CN and age ($p=0.19$) and sex ($p=0.17$) were also in the expected direction. Effect sizes estimates
138 for age and neutrophils were also consistent with prior literature [22] (Supp. Table 1). Based on variance
139 explained from previous studies, the current study was only powered to detect a significant effect for
140 neutrophil count. For all downstream analyses, mtDNA-CN was the standardized residual from a linear
141 regression model adjusted for age, sex, cell counts, ischemic time, and cohort (see **Methods**).

142

143 ***Association of mtDNA-CN derived from whole blood with gene expression in blood***

144 A priori, we expect that mitochondrially encoded gene expression would be positively correlated with
145 mtDNA-CN. Likewise, multiple nuclear encoded genes are involved in the regulation of mtDNA
146 replication, and thus, expression levels of these genes are expected to be correlated with mtDNA-CN
147 [23,24]. We therefore evaluated the associations between mtDNA-CN and expression of these two
148 classes of genes, correcting for cohort, sample ischemic time, genotyping PCs, age, race, and surrogate
149 variables derived from RNA-sequencing data to capture known and hidden confounders (Supp. Fig. 2)
150 [25].

151 To minimize the potential impact of outliers, we performed an inverse normal transformation on both
152 the mtDNA-CN metric and the gene expression values. To evaluate the association between mtDNA-CN
153 and mitochondrial RNA (mtRNA) levels, we used the median gene expression value calculated from
154 scaled expression values across 36 mtDNA-encoded genes that passed expression thresholds (see
155 **Methods**).

156 We observed a highly significant association between mtDNA-CN and overall mtRNA expression
 157 ($p=9.10e-9$) (Table 1), with 33 out of 36 individual mtDNA-encoded genes nominally significant ($p<0.05$)
 158 (Supp. Fig. 3).

159
 160 **Table 1. Blood-derived mtDNA-CN is positively associated with gene expression for mitochondrially**
 161 **encoded genes and nuclear encoded genes required for mtDNA replication.**

Gene	Effect size estimate	Standard error	P-value
Scaled mtRNA median	0.15	0.03	9.10e-09
mtDNA replication machinery			
POLG	0.02	0.01	0.025
POLG2	0.06	0.02	4.08e-04
TWNK	0.03	0.02	0.11
SSBP1	0.06	0.01	1.38e-04
PRIMPOL	0.04	0.02	0.020
DNA2	0.05	0.02	0.010
MGME1	0.04	0.02	0.048
RNASEH1	0.06	0.02	2.51e-04
mtDNA transcription machinery			
TFAM	0.06	0.01	1.83e-04
TEFM	0.03	0.02	0.05
TFB2M	0.03	0.02	0.028
POLRMT	0.01	0.01	0.19
Nucleotide metabolism genes			
TK2	0.02	0.02	0.11
DGUOK	0.06	0.02	6.39e-04
RRM2B	0.04	0.01	0.006
TYMP	0.02	0.02	0.29
SLC25A4	0.08	0.03	0.003

† Genes from Rusecka et al.

162 **Effect size estimates represent the change in gene expression, in standard deviation units, associated**
 163 **with a 1 standard deviation increase in blood-derived mtDNA-CN. Mitochondrially encoded genes are**
 164 **represented as the median of the scaled mtRNA expression of the 36 genes with detectable**
 165 **expression. Genes required for mtDNA replication were obtained from Rusecka et al [24].**
 166

167 In addition to genes coding directly for mtDNA replication machinery, genes involved in mtDNA
 168 transcription and nucleotide metabolism are also required for mtDNA replication. The mtDNA
 169 transcription machinery provides the RNA primers used in mtDNA replication and nucleotides are

170 needed to synthesize new mtDNA molecules. Of the 17 mtDNA major replication genes tested [24], all
171 were positively associated with mtDNA-CN, as would be expected based on gene function; 8 of them
172 were nominally significant ($p < 0.05$), and were 4 significant after Bonferroni correction ($p < 2.94e-3$) for
173 multiple testing (Table 1).

174 To identify additional genes and pathways associated with mtDNA-CN, we performed a transcriptome-
175 wide analysis. There was an overall inflation of test statistics, which we quantified using the genomic
176 inflation factor ($\lambda = 4.71$) [26]. Two-stage permutation testing demonstrated no inflation in null
177 datasets, suggesting that this inflation represents a true global association between blood-derived
178 mtDNA-CN and gene expression (Supp. Fig. 4).

179 When stratified by gene functional categories [27], all categories showed elevated test statistics, but
180 protein-coding genes were the most enriched ($\lambda = 7.44$) (Fig. 1). Gene expression levels of most of
181 the nominally significant genes were positively correlated with mtDNA-CN (7769 genes with positive t -
182 values vs. 285 genes with negative t -values). While much of this positive skewing is due to correlated
183 gene expression, permuted datasets demonstrate that this positive shift is significant ($P < 0.001$, Supp.
184 Fig. 5), perhaps reflecting a more active transcriptional state associated with higher mtDNA-CN. Only
185 two negatively associated genes passed permutation cutoff ($p = 2.7e-6$), *CAMP* ($p = 1.58e-8$) and *PGLYRP1*
186 ($p = 1.78e-7$), both of which are involved in innate immunity.

187

188 ***Gene set enrichment analysis uncovers gene regulatory networks in whole blood***

189 To identify specific molecular pathways, transcription factors, and gene ontologies associated with
190 mtDNA-CN in whole blood, we performed gene set enrichment analyses [28] using gene sets obtained
191 from the Molecular Signatures database (MSigDB) [29–33]. Previous studies have shown that cross-
192 mappability can lead to false pseudogene positives in eQTL association studies [34]; we therefore

193 excluded pseudogenes from subsequent analyses. Significantly associated KEGG pathways included
 194 “Spliceosome” ($p=1.03e-8$) and “Ubiquitin-mediated proteolysis” ($p=2.4e-10$) (Table 2).

195

196 **Table 2. Top 5 genes that were most significantly associated with mtDNA-CN within the “Spliceosome”**
 197 **and “Ubiquitin-mediated proteolysis” KEGG pathways.**

Gene	Effect size estimate	Standard error	P-value
Spliceosome genes			
TRA2A	0.11	0.01	2.99e-14
LSM6	0.11	0.02	3.75e-10
HNRNPA1L2	0.12	0.02	2.07e-08
SRSF8	0.10	0.02	2.24e-07
NCBP2	0.06	0.01	6.60e-07
Ubiquitin-mediated proteolysis genes			
UBE2B	0.12	0.02	1.20e-13
ELOC	0.08	0.01	2.02e-08
UBE2I	0.09	0.02	6.26e-08
CUL1	0.07	0.01	9.73e-08
UBE2K	0.07	0.01	1.32e-07

198 **Effect size estimates represent the change in gene expression, in standard deviation units, associated**
 199 **with a 1 standard deviation increase in blood-derived mtDNA-CN.**

200

201 A number of transcription factor target sequences were also significantly enriched, including those for
 202 ELK1 ($p=8.58e-66$), NRF1 ($p=1.76e-35$), GABPB ($p=3.54e-21$), YY1 ($p=3.14e-19$), and E4F1 ($p=3.98e-15$).
 203 All of these transcription factors regulate genes that play a role in mitochondrial function [35–39]. Gene
 204 expression levels of these transcription factors were all positively correlated with mtDNA-CN, with 5 out
 205 of 6 nominally significant, and 3 remaining significant after Bonferroni correction ($p<8.33e-3$) (Table 3).

206

207 **Table 3. Transcription factors whose targets are enriched for association with blood-derived mtDNA-**
 208 **CN are nearly all nominally significantly associated with blood-derived mtDNA-CN.**

Gene	Effect size estimate (gene expression)	Standard error (gene expression)	P-value (gene expression)	P-value (enriched target sequences)
NRF1	0.03	0.02	0.07	1.76e-35
YY1	0.07	0.01	1.78e-06	3.14e-19

Gene	Effect size estimate (gene expression)	Standard error (gene expression)	P-value (gene expression)	P-value (enriched target sequences)
GABPB2	0.09	0.02	1.51e-09	3.54e-21
GABPB1	0.03	0.01	0.048	3.54e-21
E4F1	0.05	0.01	2.01e-04	3.98e-15
ELK1	0.04	0.02	0.021	8.58e-66

209 **Effect size estimates, standard errors, and p-values from a linear regression between transcription**
210 **factor gene expression and blood-derived mtDNA-CN. Transcription factors shown are those whose**
211 **targets were significantly enriched for association with blood-derived mtDNA-CN.**
212

213 Many mitochondrially-related cellular component gene ontology (GO) terms were significant, including
214 “Mitochondrion” ($p=7.77e-23$), “Mitochondrial part” ($p=2.79e-15$), and “Mitochondrion organization”
215 ($p=2.87e-14$) (Fig. 2) [40]. Additional significantly associated GO terms included “ubiquitin ligase
216 complex” ($p=6.6e-18$) and “spliceosomal complex” ($p=4.46e-14$), supporting the KEGG pathway findings.
217 Genes with substantial evidence of mitochondrial localization, determined through integration of
218 several genome-scale datasets, were obtained from MitoCarta2.0 and demonstrated significant
219 enrichment ($p=8.22e-21$) [41].

220

221 ***Cross-tissue analysis reveals associations between gene expression in multiple tissues and blood-***
222 ***derived mtDNA-CN***

223 mtDNA-CN measured in blood has been associated with a number of aging-related diseases including
224 chronic kidney disease, heart failure, and diabetes [10,42,43]. Given that these diseases primarily
225 manifest in non-blood tissues, we evaluated associations between blood-derived mtDNA-CN and gene
226 expression measured from 47 additional tissues that had greater than 50 samples after filtering.

227 Though blood-derived mtDNA-CN appears to be associated with gene expression in other tissues, we did
228 not observe a significant association between blood-derived mtDNA-CN and scaled mtRNA gene
229 expression in any tissue other than blood, and only 2 out of 47 tested tissues had nominally significant
230 associations between tissue-specific scaled mtRNA expression and blood-derived mtDNA-CN (Uterus [p

231 = 0.004], Heart – Left Ventricle [$p = 0.017$]). (Supp. Table 2). However, mtRNA expression for 35/47 non-
232 blood tissues was positively associated with blood mtDNA-CN, which is more than what would be
233 expected by chance ($p < 0.001$). This suggests that while our study may be underpowered to detect a
234 significant association in individual tissues due to small sample sizes, mtDNA-CN measured in blood is
235 broadly correlated with mtDNA-CN in other tissues.

236 We calculated genomic inflation factors for each tissue to quantify test statistic inflation. Genomic
237 inflation factors were elevated across multiple non-blood tissues, suggesting that blood-derived mtDNA-
238 CN was broadly associated with gene expression in other tissues (Fig. 3). To determine true signal from
239 noise, we performed 100 two-stage permutations for each tissue and obtained a genomic inflation
240 factor lambda cutoff of >1.20 representing a significant elevation of lambda (study-wide $p < 0.05$). Using
241 this cutoff, we identified 30 non-blood tissues with a global inflation of test statistics [Supp. Table 3].

242 Other than blood, the most strongly enriched tissue was the putamen region of the brain, with a lambda
243 of 3.27. We note that the two cell lines, EBV transformed lymphocytes (lambda=0.84) and cultured
244 fibroblasts (lambda=0.84), showed no global inflation of test statistics, suggesting that blood-derived
245 mtDNA-CN loses its association with gene expression after the cell-culturing process.

246 To examine the similarity of associations of mtDNA-CN observed in blood with other tissues, we
247 calculated Spearman's rank correlation coefficients between effect estimates for blood-derived mtDNA-
248 CN on blood gene expression (β_{blood}) and effect estimates for blood-derived mtDNA-CN on gene
249 expression in other tissues (β_{tissue}). All genes that passed a permutation cutoff for significance in blood
250 ($p = 2.7e-6$, 721 genes total) were included. To distinguish tissues with correlations more extreme than
251 baseline, we calculated reference correlations between blood and other tissues for randomly selected
252 sets of genes. 26 tissues had observed values that were more extreme than the random gene sets
253 (Supp. Table 4). Of these 26 tissues, 20 were among the 30 tissues with significantly inflated lambdas.

254 To identify pathways associated with mtDNA-CN across multiple tissues, we performed gene set
 255 enrichment analysis in each of the 30 tissues with a significant genomic inflation factor. Multiple terms
 256 were significant in greater than one tissue (Table 4), including terms related to oxidative
 257 phosphorylation and mitochondria, suggesting that mtDNA-CN derived from blood can reflect
 258 mitochondrial function occurring in other tissues.

259

260 **Table 4. Pathways, transcription factor targets, and GO terms significantly enriched in multiple tissues.**

Pathway	Number of significant tissues
Transcription factors	
SCGGAAGY_ELK1_Q2	18
RCGCANGCGY_NRF1_Q6	12
GCCATNTTG_YY1_Q6	8
TGCGCANK_UNKNOWN	8
MGGAAGTG_GABP_B	7
GO terms	
GO_RNA_BINDING	16
GO_CATALYTIC_COMPLEX	14
GO_CELLULAR_MACROMOLECULE_LOCALIZATION	13
GO_INTRACELLULAR_TRANSPORT	13
GO_MACROMOLECULE_CATABOLIC_PROCESS	12
KEGG terms	
KEGG_RIBOSOME	8
KEGG_HUNTINGTONS_DISEASE	4
KEGG_OXIDATIVE_PHOSPHORYLATION	4
KEGG_ALZHEIMERS_DISEASE	3
KEGG_PARKINSONS_DISEASE	3
Mitochondrial terms	
GO_MITOCHONDRIAL_ENVELOPE	8
GO_MITOCHONDRIAL_PART	8
GO_MITOCHONDRION	7
GO_MITOCHONDRION_ORGANIZATION	4
GO_MITOCHONDRIAL_PROTEIN_COMPLEX	3

261 **The top 5 terms for each category that were significantly enriched in multiple tissues are shown.**

262 ELK1 transcription factor binding sites were significantly enriched in 17 of the 30 significant tissues, and
 263 were also significant in whole blood, suggesting that mtDNA-CN may regulate ELK1 or vice versa. We
 264 note that gene expression for ELK1 was nominally significantly associated ($p < 0.05$) with blood-derived

265 mtDNA-CN in 12 of the 18 tissues for which ELK1 targets were significantly enriched (Supp. Fig. 6). Effect
266 estimates for ELK1 targets were generally consistent with the directionality of ELK1 effect estimates. For
267 example, in blood, where ELK1 expression is positively associated with mtDNA-CN, 747/750 (99.6%)
268 nominally significant ELK1 target genes were positively associated. On the other hand, mtDNA-CN was
269 negatively associated with nerve ELK1 gene expression, and 204/306 (66.67%) nominally significant ELK1
270 target genes were also negatively associated. Of note, nearly all the noted transcription factors were
271 ubiquitously expressed throughout the body, except for ELK1, which is not expressed in Brain Putamen
272 or Spinal Cord (Supp. Fig. 7).

273 To identify genes driving enrichment of significant pathways in multiple tissues, we performed a random
274 effects meta-analysis for all expressed genes using effect size estimates from all 47 non-blood tissues.
275 Strikingly, genes encoding both the large and small ribosomal subunits were negatively associated with
276 blood-derived mtDNA-CN across all tested tissues, implying an inverse relationship between ribosomal
277 abundance and mitochondrial DNA quantity (Table 5).

278

279 **Table 5. Random-effects meta-analysis for genes driving the enrichment of pathways in multiple**
280 **tissues.**

Gene	Meta effect size estimate	Meta standard error	Meta p-value
ELK1 targets			
STARD3	0.05	0.00	1.49e-17
EIF5A	0.08	0.01	4.97e-17
ERH	0.07	0.01	8.82e-17
RNA-binding genes			
SUZ12	0.06	0.00	4.49e-18
C1D	0.11	0.01	8.03e-18
MRPL23	-0.09	0.01	8.37e-18
Ribosome genes			
RPL34	-0.07	0.01	8.57e-16
RPS27	-0.08	0.01	1.35e-15
RPL39	-0.08	0.01	1.16e-14
Mitochondrial part genes			
MRPL23	-0.09	0.01	8.37e-18

Gene	Meta effect size estimate	Meta standard error	Meta p-value
MTERF3	-0.06	0.00	3.12e-17
MICU3	0.09	0.01	3.34e-17

281 **Meta-analysis results are from all 47 tested tissues, excluding effects from whole blood. Top 3 most**
282 **significant genes for each pathway are shown.**
283

284 Huntington's disease (HD), Parkinson's disease (PD), and Alzheimer's disease (AD) were among the most
285 significantly associated KEGG pathways that appear in multiple tissues (Table 5). This is an intriguing
286 finding, given the known role of mitochondria in neurodegenerative disease [44].

287 While neurodegenerative disorders primarily manifest in nervous tissues [45], we observed significant
288 enrichment of disease pathways in colon, pancreas, and testis tissues. When limiting our query to brain
289 tissues, HD and PD were nominally significantly enriched in cerebellum, caudate (basal ganglia), and
290 cortex, while AD was nominally significantly enriched in cerebellum and spinal cord (Supp. Fig 8).

291

292 ***mtDNA-CN is associated with incident neurodegenerative disease in the UKBiobank***

293 To examine the association between mtDNA-CN and neurodegenerative disease risk, we used the UK
294 Biobank (UKB) [46], a prospective cohort study with whole exome sequencing for ~50,000 individuals.
295 mtDNA-CN was derived from whole exome sequencing and adjusted for sequencing artifacts, age, and
296 sex. Analysis was restricted to individuals of European descent, and individuals with blood cell type
297 count outliers were excluded. Using a Cox proportional-hazards model and adjusting for age and sex, we
298 evaluated the relative risk of neurodegenerative disease associated with mtDNA-CN. Median follow-up
299 time was approximately 10 years. Although the number of incident events was small, mtDNA-CN was
300 significantly associated with Parkinson's disease (HR=0.75, CI=0.60;0.99) and Alzheimer's disease
301 (HR=0.59, CI=0.44;0.81), and approached significance for non-Alzheimer's dementia (HR=0.81,
302 CI=0.65;1.02). Consistent with other aging-related diseases [7,9], higher mtDNA-CN was associated with
303 lower risk for developing incident neurodegenerative disease (Table 6). A combined analysis for all

304 individuals with incident neurodegenerative disease revealed a consistent strongly significant
305 association (HR=0.73, CI=0.66;0.90).

306

307 **Table 6. mtDNA-CN is associated with incident neurodegenerative disease.**

Disease	Hazard ratio	Confidence interval	Number of cases/controls	P-value
Parkinson's disease	0.75	0.60;0.99	63/39,044	0.030
Alzheimer's disease	0.59	0.44;0.81	41/39,100	0.001
Dementia (excluding AD)	0.81	0.65,1.02	74/39,048	0.074
Combined neurodegenerative disease	0.73	0.66;0.90	161/39,030	0.001

308 **Hazard ratios for incident neurodegenerative disease associate with a 1 standard deviation increase in**
309 **whole blood mtDNA-CN estimated from Cox proportional-hazards models in the UKBiobank. Analysis**
310 **was restricted to individuals of European descent, and individuals who were outliers for cell counts**
311 **were excluded from analysis.**

312

313 **DISCUSSION**

314 In this study, blood-derived mtDNA-CN was significantly associated with a host of blood-expressed
315 genes. As expected, nearly all genes involved in mtDNA replication were significantly associated with
316 mtDNA-CN in a positive direction. There was also a clear overall shift towards significant positive
317 estimates, possibly indicating that increased mtDNA-CN is reflective of a more active transcriptional
318 state. This finding is consistent with previous literature demonstrating that higher mitochondrial content
319 is correlated with increased transcriptional activity [47,48]. Strikingly, the two negatively associated
320 genes both play roles in innate immune function [41,42], suggesting that higher mtDNA-CN levels are
321 correlated with decreased immune response. Mitochondria play a role in immune responses to
322 pathogens in several ways; for example, mitochondrial DNA release from compromised mitochondria
323 can trigger an intracellular antiviral response through the cGAS/STING pathway [51], binding of viral
324 dsRNA to the mitochondrial antiviral signaling complex (MAVS) can trigger an interferon responses
325 through STAT6 activation [52], and release of mitochondrial components from cells can bind to damage-

326 associated molecular pattern (DAMP) receptors to trigger innate immune responses [53]. These novel
327 findings correlating expression of mtDNA-CN with specific immune response genes in tissues represent
328 an area for further investigation.

329 Gene set enrichment analyses revealed pathways potentially involved in mitochondrial DNA control,
330 including ubiquitin-mediated proteolysis and splicing. Supporting this finding, Guantes et. al
331 demonstrated that mitochondrial content modulates alternative splicing [47]. Additionally, we found
332 that genes expressed in whole blood that were associated with blood-derived mtDNA-CN were enriched
333 for target sequences for the ELK1, NRF1, YY1, GABPB, and E4F1 transcription factors. All of these
334 transcription factors have been implicated in mitochondrial pathways, as ELK1 is associated with the
335 mitochondrial permeability transition pore complex in neurons, NRF1 regulates expression of the
336 mitochondrial translocase TOMM34, YY1 binds to and represses mitochondrial gene expression in
337 skeletal muscle, GABPB is required for mitochondrial biogenesis, and E4F1 controls mitochondrial
338 homeostasis [35–39]. Additionally, we found significant enrichment of signal for genes implicated in
339 ubiquitin-mediated proteolysis and splicing. Given that mitochondrial quality control is regulated
340 through ubiquitination, and that nuclear-encoded spliceosomes are involved in mtRNA splicing, our
341 results likely implicate processes involved in mitochondrial DNA regulatory networks [54,55].

342 mtDNA-CN measured in one tissue has previously been found to be uncorrelated with mtDNA-CN in
343 another tissue from the same individual [56]. We found that while mtRNA transcription in individual
344 tissues was not significantly correlated with blood-derived mtDNA-CN, across all tissues, there was a
345 significant enrichment for positive associations, suggesting a weak positive correlation between blood-
346 derived mtDNA-CN and mtDNA-CN in other tissues. Moreover, we found that blood-derived mtDNA-CN
347 was associated with various biological pathways in non-blood tissues (including mitochondrial function),
348 providing a possible explanation as to why blood-derived mtDNA-CN is associated with aging-related
349 diseases that primarily manifest in non-blood tissues. Further examination of pathways significant in

350 multiple tissues revealed that ribosomal subunit genes were significantly negatively associated with
351 mtDNA-CN. While there has been conflicting evidence on the relationship between mtDNA-CN and
352 ribosomal content, our study revealed a strong inverse relationship between ribosomal DNA dosage and
353 mtDNA-CN [16,47]. Importantly, since these are statistical associations, causal directionality cannot be
354 determined between gene expression and blood-derived mtDNA-CN. Future follow-up studies are
355 needed to determine functional causality for mtDNA-CN and gene expression.

356 Strikingly, KEGG pathways that were significantly enriched in multiple tissues included Huntington's
357 disease, Alzheimer's disease, and Parkinson's disease. These aging-related neurodegenerative diseases
358 have all underlying mitochondrial pathologies [57–60] and dysregulated ubiquitination pathways [61]. In
359 particular, mtDNA-CN has been implicated in Alzheimer's disease [62–64] and cognitive function [65,66].
360 Further, the ELK1 transcription factor, whose target sequences were significantly enriched in 18 tissues,
361 plays a role in multiple neurodegenerative diseases [67]. Finally, after finding that blood-derived
362 mtDNA-CN was associated with expression of neurodegenerative disease genes, we used an
363 independent dataset, the UK Biobank, and found that mtDNA-CN was significantly associated with
364 incident neurodegenerative disease risk. Notably, the population of individuals used for the UK Biobank
365 analyses is biased towards fewer smokers and fewer prevalent Parkinson's events [68], which may
366 impact the generalizability of our results. Despite this caveat, we show that blood-derived mtDNA-CN is
367 significantly associated with gene expression from tissues across the body, and that higher mtDNA-CN is
368 associated with decreased incident neurodegenerative disease risk.

369

370 **METHODS**

371 ***GTEX Sample acquisition***

372 Whole genome sequences were downloaded from the GTEx version 8 cloud repository on 11/18/2020.

373 RNA-sequencing data used for analyses was downloaded from the GTEx portal

374 (<http://gtexportal.org/home/datasets>) on 06/18/2019 and phenotypes were obtained from dbGaP
375 (phs000424.v8.p2).

376 ***Estimation of mtDNA-CN***

377 Samtools version 1.9 [69] was used to count the number of mitochondrial, unaligned, and total reads for
378 each whole genome sequence. mtDNA-CN was estimated as the number of mitochondrial reads divided
379 by the difference between the number of total reads and the number of unaligned reads to obtain a
380 ratio of mtDNA to nuclear DNA. Whole genome is a highly accurate method for estimation of mtDNA-CN
381 [22,56].

382 ***Correcting mtDNA-CN for covariates***

383 All statistical analyses were performed with R version 3.6.1. Cell type composition for whole blood
384 samples was determined from RNA-sequencing using xCell [19], only allowing for deconvolution of cell
385 types found in blood. A stepwise regression in both directions was used to select appropriate cell types
386 to correct mtDNA-CN. To avoid model overfitting, correlated cell types ($R > 0.8$) were removed. The final
387 model used to adjust mtDNA-CN included neutrophils, hematopoietic stem cells, megakaryocytes,
388 subject cohort, ischemic time, age, and sex. Power calculations were performed using R^2 values from
389 previous studies using the pwr package [22].

390 ***Filtering pipeline***

391 A batch effect due to sample collection and/or sequencing methods resulted in significantly altered
392 mtDNA-CN for individuals who were sequenced prior to January 2013. To keep this from confounding
393 the analysis, we excluded subjects with whole genome sequencing prior to January 2013 (Supp. Fig. 1).
394 Individuals who had greater than 5×10^7 unaligned whole genome sequence reads were also omitted
395 from the analysis. Cell type outliers who were greater than 3 standard deviations (SDs) from the mean
396 were excluded as well. Only one individual remained from the surgical cohort after filtering and
397 therefore was also removed (Supp. Fig. 9).

398 ***RNA-sequencing pipeline***

399 GTEx version 8 RNA-sequencing data was downloaded from the GTEx website in transcripts per million
400 (TPMs) and normalized using the trimmed mean of M-values method prior to analyses [70,71]. Genes
401 with expression greater than 0.1 TPMs for at least 20% of samples were retained for analysis. To identify
402 potential hidden confounders, we used surrogate variable analysis (SVA), protecting mtDNA-CN from SV
403 generation [25]. SVs were associated with known covariates in the data, such as whether individuals
404 were in the postmortem or the organ donor cohorts (Supp. Fig. 2). Individuals who were greater than 3
405 standard deviations from the mean for the first ten SVs were omitted from analysis. SV generation was
406 performed iteratively 3 times.

407 ***Linear model for evaluating associations***

408 To reduce the influence of outliers, both the gene expression metric and the mtDNA-CN metric were
409 inverse normal transformed prior to linear regression. We then tested for association using multiple
410 linear regression, with mtDNA-CN as the predictor and gene expression as the outcome, correcting for
411 SVs, sex, cohort, race, ischemic time, and the first three genotyping principal components.

412 ***Genomic inflation factor calculation***

413 Genomic inflation factors were calculated by squaring z-scores to obtain chi-squared values. The median
414 observed chi-squared value was divided by the expected median to obtain lambda [26].

415 ***Two-stage permutations***

416 To determine an appropriate p-value cutoff, we created null datasets for permutation testing. First, a
417 multiple linear regression model for the alternate hypothesis was used to obtain gene expression
418 residuals. Second, a multiple linear regression model for the null hypothesis was used to obtain
419 estimates for each gene. Residuals from the alternate model were then permuted and added to effect
420 estimates from the null model to create null datasets. Permuted gene expression data was then tested
421 for association with mtDNA-CN. Unless otherwise stated, permutations were performed 100 times.

422 Minimum p-values from each permuted dataset were obtained, and the 5th lowest p-value was utilized
423 as a permutation cutoff.

424 ***Annotation of gene categories***

425 Gene annotations were downloaded from Gencode [27]. Test statistics were then stratified by gene type
426 and observed and expected distributions were generated for each category.

427 ***Overrepresentation of positive beta estimates***

428 Percentage of positive effect estimates was calculated using all nominally significant genes in blood,
429 dividing the number of nominally significant genes with positive effect estimates by the total number of
430 nominally significant genes. Percentages for null distributions were calculated using 1000 permutations
431 generated using the two-stage permutation method described above.

432 ***Gene set enrichment analysis***

433 To examine enrichment for genes in specific pathways, gene sets for KEGG pathways, transcription
434 factor target sequences, and gene ontologies were downloaded from the Molecular Signatures database
435 [25,27,49]. Then, using the absolute value of the t-scores from the regression model with mtDNA-CN,
436 we performed a t-test of t-scores for genes in a specific pathway versus genes that were not contained
437 in the pathway. Permutations using randomized t-scores were used to determine appropriate cutoffs for
438 significance. To confirm that results were not driven by individual genes in a pathway with very large t-
439 scores, we also performed t-tests using ranked t-scores as opposed to absolute value t-scores.

440 ***REVIGO trimming and visualization of GO terms***

441 For visualization of significantly enriched GO terms and elimination of redundant GO terms, REVIGO
442 (<http://revigo.irb.hr/>) was used with the default settings except for the allowed similarity, which was
443 set to medium (0.7) [40].

444 ***Testing for associations between blood-derived mtDNA-CN and gene expression in other tissues***

445 Filtering parameters and models for testing the association of blood-derived mtDNA-CN with gene
446 expression in other tissues were identical to the pipeline used in whole blood. Only tissues with greater
447 than 50 observations after filtering were tested. For tissues that had no variation in covariates,
448 covariates were dropped from the linear model (i.e. sex was not used in the model for testing gene
449 expression in reproductive organs and cohort was not used in the model for brain tissues).

450 ***Spearman correlations for effect estimates with whole blood***

451 All significant genes in whole blood that passed the permutation cutoff ($p=2.7 \times 10^{-6}$) were used for
452 testing. Spearman correlations between effect estimates in blood and effect estimates in other tissues
453 were calculated. To compare correlations for genes significant in blood with baseline correlation, we
454 randomly selected 100 random genes and calculated correlations between blood estimates and specific
455 tissue estimates for those genes. We repeated this random selection 100 times to generate multiple
456 baseline correlation measures.

457 ***Meta-analysis of genes driving specific ontologies***

458 To calculate meta-analysis effect estimates and p-values, the R '*meta*' package [73] was used to perform
459 a random-effects meta-analysis using all effect estimates and p-values for all tissues, excluding results
460 from whole blood.

461 ***Association of mtDNA-CN with neurodegenerative disease in UKB***

462 Samtools version 1.9 was used to extract read summary statistics from 49,997 UK biobank whole exome
463 sequences. An in-house perl script was then used to aggregate summary statistics into the number of
464 total, mapped, unmapped, autosomal, chromosome X, chromosome Y, mitochondrial, random,
465 unknown, decoy1, and decoy2 reads. 10-fold cross validation was used to select linear regression
466 covariates to adjust the number of mitochondrial reads for. After correcting for these potential technical
467 artifacts, this metric was then adjusted for age and sex. Cell type outliers were excluded from the
468 dataset, and subsequent analyses were restricted to individuals of European descent. A Cox

469 proportional-hazards model was used to evaluate the association between mtDNA-CN and time to
470 incident neurodegenerative disease, adjusting for age and sex.

471
472

473 **DECLARATIONS**

474 ***Ethics approval and consent to participate***

475 Approval access for the datasets in this study was obtained from the GTEx and UKBiobank resources.

476 ***Consent for publication***

477 **Not applicable**

478 ***Availability of data and materials***

479 RNA-sequencing data used for analyses was downloaded from the GTEx portal

480 (<http://gtexportal.org/home/datasets>) on 06/18/2019 and phenotypes were obtained from dbGaP

481 (phs000424.v8.p2). Aligned whole genome sequences were downloaded from google cloud. UKBiobank

482 data was accessed under application number 17731. All in-house scripts can be found in the following

483 Github repository: https://github.com/syyang93/mtDNA_GE_scripts.

484 ***Competing interests***

485 The authors declare that they have no competing interests.

486 ***Funding***

487 This work was supported by grants R01HL13573 and R01HL144569.

488 ***Authors' contributions***

489 Concept and design: Yang, Arking

490 Acquisition, analysis, or interpretation of data: Yang, Castellani, Longchamps, Pillalamarri, Arking

491 Drafting manuscript: Yang, Arking

492 Critical revision of the manuscript: Yang, Castellani, Longchamps, Pillalamarri, O'Rourke, Guallar, Arking

493 Obtaining funding: Arking

494 **Acknowledgements**

495 This research was conducted using data from the Genotype-Tissue Expression (GTEx) project (dbGaP
496 accession: phs000424.v8.p2). The GTEx project was supported by the Common Fund of the Office of the
497 Director of the National Institutes of Health, and by NCI, NHGRI, NHLBI, NIDA, NIMH, and NINDS.
498 This research was also conducted using the UK Biobank Resource under Application Number 17731.

499 **REFERENCES**

- 500 1. Wai T, Ao A, Zhang X, Cyr D, Dufort D, Shoubridge EA. The role of mitochondrial DNA copy number in
501 mammalian fertility. *Biol Reprod.* 2010;83:52–62.
- 502 2. Clay Montier LL, Deng J, Bai Y. Number matters: control of mammalian mitochondrial DNA copy
503 number. *J Genet Genomics.* 2009;36:125–31.
- 504 3. Miller FJ, Rosenfeldt FL, Zhang C, Linnane AW, Nagley P. Precise determination of mitochondrial DNA
505 copy number in human skeletal and cardiac muscle by a PCR-based assay: lack of change of copy
506 number with age. *Nucleic Acids Res.* 2003;31:e61.
- 507 4. Herst PM, Rowe MR, Carson GM, Berridge MV. Functional Mitochondria in Health and Disease. *Front*
508 *Endocrinol (Lausanne)* [Internet]. 2017 [cited 2020 May 28];8. Available from:
509 <https://www.ncbi.nlm.nih.gov/pmc/articles/PMC5675848/>
- 510 5. Malik AN, Czajka A. Is mitochondrial DNA content a potential biomarker of mitochondrial
511 dysfunction? *Mitochondrion.* 2013;13:481–92.
- 512 6. Castellani CA, Longchamps RJ, Sun J, Guallar E, Arking DE. Thinking outside the nucleus: Mitochondrial
513 DNA copy number in health and disease. *Mitochondrion.* 2020;53:214–23.
- 514 7. Ashar FN, Moes A, Moore AZ, Grove ML, Chaves PHM, Coresh J, et al. Association of mitochondrial
515 DNA levels with frailty and all-cause mortality. *J Mol Med.* 2015;93:177–86.
- 516 8. Association between Mitochondrial DNA Copy Number in Peripheral Blood and Incident CKD in the
517 Atherosclerosis Risk in Communities Study | American Society of Nephrology [Internet]. [cited 2020 Feb
518 17]. Available from: <https://jasn.asnjournals.org/content/27/8/2467>
- 519 9. Ashar FN, Zhang Y, Longchamps RJ, Lane J, Moes A, Grove ML, et al. Association of Mitochondrial DNA
520 Copy Number With Cardiovascular Disease. *JAMA Cardiol.* 2017;2:1247–55.
- 521 10. Huang J, Tan L, Shen R, Zhang L, Zuo H, Wang DW. Decreased Peripheral Mitochondrial DNA Copy
522 Number is Associated with the Risk of Heart Failure and Long-term Outcomes. *Medicine (Baltimore)*
523 [Internet]. 2016 [cited 2020 Feb 17];95. Available from:
524 <https://www.ncbi.nlm.nih.gov/pmc/articles/PMC4839823/>
- 525 11. Ali AT, Boehme L, Carbajosa G, Seitan VC, Small KS, Hodgkinson A. Nuclear genetic regulation of the
526 human mitochondrial transcriptome. McCarthy MI, Battle A, Arking D, editors. *eLife.* 2019;8:e41927.

- 527 12. Lee WT, Sun X, Tsai T-S, Johnson JL, Gould JA, Garama DJ, et al. Mitochondrial DNA haplotypes
528 induce differential patterns of DNA methylation that result in differential chromosomal gene expression
529 patterns. *Cell Death Discov.* 2017;3:17062.
- 530 13. Sun X, St John JC. Modulation of mitochondrial DNA copy number in a model of glioblastoma induces
531 changes to DNA methylation and gene expression of the nuclear genome in tumours. *Epigenetics*
532 *Chromatin.* 2018;11:53.
- 533 14. Reznik E, Miller ML, Şenbabaoğlu Y, Riaz N, Sarungbam J, Tickoo SK, et al. Mitochondrial DNA copy
534 number variation across human cancers. *Elife.* 2016;5.
- 535 15. Castellani CA, Longchamps RJ, Sumpter JA, Newcomb CE, Lane JA, Grove ML, et al. Mitochondrial
536 DNA Copy Number (mtDNA-CN) Can Influence Mortality and Cardiovascular Disease via Methylation of
537 Nuclear DNA CpGs [Internet]. *Genomics*; 2019 Jun. Available from:
538 <http://biorxiv.org/lookup/doi/10.1101/673293>
- 539 16. Gibbons JG, Branco AT, Yu S, Lemos B. Ribosomal DNA copy number is coupled with gene expression
540 variation and mitochondrial abundance in humans. *Nature Communications.* 2014;5:1–12.
- 541 17. Lonsdale J, Thomas J, Salvatore M, Phillips R, Lo E, Shad S, et al. The Genotype-Tissue Expression
542 (GTEx) project. *Nat Genet.* 2013;45:580–5.
- 543 18. Zhang R, Wang Y, Ye K, Picard M, Gu Z. Independent impacts of aging on mitochondrial DNA quantity
544 and quality in humans. *BMC Genomics* [Internet]. 2017 [cited 2020 Mar 4];18. Available from:
545 <https://www.ncbi.nlm.nih.gov/pmc/articles/PMC5697406/>
- 546 19. Aran D, Hu Z, Butte AJ. xCell: digitally portraying the tissue cellular heterogeneity landscape.
547 *Genome Biol.* 2017;18:220.
- 548 20. Moore AZ, Ding J, Tuke MA, Wood AR, Bandinelli S, Frayling TM, et al. Influence of cell distribution
549 and diabetes status on the association between mitochondrial DNA copy number and aging phenotypes
550 in the InCHIANTI study. *Aging Cell* [Internet]. 2018 [cited 2020 Feb 17];17. Available from:
551 <https://www.ncbi.nlm.nih.gov/pmc/articles/PMC5770782/>
- 552 21. Mengel-From J, Thinggaard M, Dalgård C, Kyvik KO, Christensen K, Christiansen L. Mitochondrial DNA
553 copy number in peripheral blood cells declines with age and is associated with general health among
554 elderly. *Hum Genet.* 2014;133:1149–59.
- 555 22. Longchamps RJ, Castellani CA, Yang SY, Newcomb CE, Sumpter JA, Lane J, et al. Evaluation of
556 mitochondrial DNA copy number estimation techniques. *PLOS ONE.* 2020;15:e0228166.
- 557 23. Garcia I, Jones E, Ramos M, Innis-Whitehouse W, Gilkerson R. The little big genome: the organization
558 of mitochondrial DNA. *Front Biosci (Landmark Ed).* 2017;22:710–21.
- 559 24. Rusecka J, Kaliszewska M, Bartnik E, Tońska K. Nuclear genes involved in mitochondrial diseases
560 caused by instability of mitochondrial DNA. *J Appl Genet.* 2018;59:43–57.
- 561 25. Leek JT, Storey JD. Capturing heterogeneity in gene expression studies by surrogate variable analysis.
562 *PLoS Genet.* 2007;3:1724–35.

- 563 26. Devlin B, Roeder K. Genomic control for association studies. *Biometrics*. 1999;55:997–1004.
- 564 27. Harrow J, Frankish A, Gonzalez JM, Tapanari E, Diekhans M, Kokocinski F, et al. GENCODE: The
565 reference human genome annotation for The ENCODE Project. *Genome Res*. 2012;22:1760–74.
- 566 28. Irizarry RA, Wang C, Zhou Y, Speed TP. Gene Set Enrichment Analysis Made Simple. *Stat Methods*
567 *Med Res*. 2009;18:565–75.
- 568 29. Liberzon A, Subramanian A, Pinchback R, Thorvaldsdóttir H, Tamayo P, Mesirov JP. Molecular
569 signatures database (MSigDB) 3.0. *Bioinformatics*. Oxford Academic; 2011;27:1739–40.
- 570 30. Ashburner M, Ball CA, Blake JA, Botstein D, Butler H, Cherry JM, et al. Gene Ontology: tool for the
571 unification of biology. *Nat Genet*. 2000;25:25–9.
- 572 31. Xie X, Lu J, Kulbokas EJ, Golub TR, Mootha V, Lindblad-Toh K, et al. Systematic discovery of regulatory
573 motifs in human promoters and 3' UTRs by comparison of several mammals. *Nature*. Nature Publishing
574 Group; 2005;434:338–45.
- 575 32. The Gene Ontology Resource: 20 years and still GOing strong. *Nucleic Acids Res*. Oxford Academic;
576 2019;47:D330–8.
- 577 33. Meng H, Yaari G, Bolen CR, Avey S, Kleinstein SH. Gene set meta-analysis with Quantitative Set
578 Analysis for Gene Expression (QuSAGE). *PLOS Computational Biology*. Public Library of Science;
579 2019;15:e1006899.
- 580 34. Saha A, Battle A. False positives in trans-eQTL and co-expression analyses arising from RNA-
581 sequencing alignment errors. *F1000Res* [Internet]. 2019 [cited 2020 Mar 4];7. Available from:
582 <https://www.ncbi.nlm.nih.gov/pmc/articles/PMC6305209/>
- 583 35. Chen F, Zhou J, Li Y, Zhao Y, Yuan J, Cao Y, et al. YY1 regulates skeletal muscle regeneration through
584 controlling metabolic reprogramming of satellite cells. *EMBO J*. 2019;38.
- 585 36. Barrett LE, Bockstaele EJ, Sul JY, Takano H, Haydon PG, Eberwine JH. Elk-1 associates with the
586 mitochondrial permeability transition pore complex in neurons. *PNAS*. National Academy of Sciences;
587 2006;103:5155–60.
- 588 37. Blesa JR, Prieto-Ruiz JA, Abraham BA, Harrison BL, Hegde AA, Hernández-Yago J. NRF-1 is the major
589 transcription factor regulating the expression of the human TOMM34 gene. *Biochem Cell Biol*.
590 2008;86:46–56.
- 591 38. Yang Z-F, Drumea K, Mott S, Wang J, Rosmarin AG. GABP transcription factor (nuclear respiratory
592 factor 2) is required for mitochondrial biogenesis. *Mol Cell Biol*. 2014;34:3194–201.
- 593 39. Rodier G, Kirsh O, Baraibar M, Houlès T, Lacroix M, Delpech H, et al. The Transcription Factor E4F1
594 Coordinates CHK1-Dependent Checkpoint and Mitochondrial Functions. *Cell Reports*. 2015;11:220–33.
- 595 40. Supek F, Bošnjak M, Škunca N, Šmuc T. REVIGO Summarizes and Visualizes Long Lists of Gene
596 Ontology Terms. *PLOS ONE*. Public Library of Science; 2011;6:e21800.

- 597 41. MitoCarta2.0: an updated inventory of mammalian mitochondrial proteins [Internet]. [cited 2020
598 Feb 25]. Available from: <https://www.ncbi.nlm.nih.gov/pmc/articles/PMC4702768/>
- 599 42. Al-Kafaji G, Aljadaan A, Kamal A, Bakhiet M. Peripheral blood mitochondrial DNA copy number as a
600 novel potential biomarker for diabetic nephropathy in type 2 diabetes patients. *Exp Ther Med*.
601 2018;16:1483–92.
- 602 43. Tin A, Grams ME, Ashar FN, Lane JA, Rosenberg AZ, Grove ML, et al. Association between
603 Mitochondrial DNA Copy Number in Peripheral Blood and Incident CKD in the Atherosclerosis Risk in
604 Communities Study. *J Am Soc Nephrol*. 2016;27:2467–73.
- 605 44. Reddy PH. The role of mitochondria in neurodegenerative diseases: mitochondria as a therapeutic
606 target in Alzheimer’s disease. *CNS Spectr*. 2009;14:8–18.
- 607 45. Wood LB, Winslow AR, Strasser SD. *Systems Biology of Neurodegenerative Diseases*. *Integr Biol*
608 (Camb). 2015;7:758–75.
- 609 46. Bycroft C, Freeman C, Petkova D, Band G, Elliott LT, Sharp K, et al. The UK Biobank resource with
610 deep phenotyping and genomic data. *Nature*. Nature Publishing Group; 2018;562:203–9.
- 611 47. Guantes R, Rastrojo A, Neves R, Lima A, Aguado B, Iborra FJ. Global variability in gene expression and
612 alternative splicing is modulated by mitochondrial content. *Genome Res*. 2015;25:633–44.
- 613 48. Márquez-Jurado S, Díaz-Colunga J, das Neves RP, Martínez-Lorente A, Almazán F, Guantes R, et al.
614 Mitochondrial levels determine variability in cell death by modulating apoptotic gene expression. *Nature*
615 *Communications*. Nature Publishing Group; 2018;9:389.
- 616 49. Osanai A, Sashinami H, Asano K, Li S-J, Hu D-L, Nakane A. Mouse Peptidoglycan Recognition Protein
617 PGLYRP-1 Plays a Role in the Host Innate Immune Response against *Listeria monocytogenes* Infection.
618 *Infection and Immunity*. American Society for Microbiology Journals; 2011;79:858–66.
- 619 50. Gombart AF, Borregaard N, Koeffler HP. Human cathelicidin antimicrobial peptide (CAMP) gene is a
620 direct target of the vitamin D receptor and is strongly up-regulated in myeloid cells by 1,25-
621 dihydroxyvitamin D3. *FASEB J*. 2005;19:1067–77.
- 622 51. West AP, Houry-Hanold W, Staron M, Tal MC, Pineda CM, Lang SM, et al. Mitochondrial DNA stress
623 primes the antiviral innate immune response. *Nature*. 2015;520:553–7.
- 624 52. Chen H, Sun H, You F, Sun W, Zhou X, Chen L, et al. Activation of STAT6 by STING is critical for
625 antiviral innate immunity. *Cell*. 2011;147:436–46.
- 626 53. Nakahira K, Hisata S, Choi AMK. The Roles of Mitochondrial Damage-Associated Molecular Patterns
627 in Diseases. *Antioxid Redox Signal*. 2015;23:1329–50.
- 628 54. Bragoszewski P, Turek M, Chacinska A. Control of mitochondrial biogenesis and function by the
629 ubiquitin–proteasome system. *Open Biol* [Internet]. 2017 [cited 2020 Mar 31];7. Available from:
630 <https://www.ncbi.nlm.nih.gov/pmc/articles/PMC5413908/>

- 631 55. Herai RH, Negraes PD, Muotri AR. Evidence of nuclei-encoded spliceosome mediating splicing of
632 mitochondrial RNA. *Hum Mol Genet.* 2017;26:2472–9.
- 633 56. Wachsmuth M, Hübner A, Li M, Madea B, Stoneking M. Age-Related and Heteroplasmy-Related
634 Variation in Human mtDNA Copy Number. *PLOS Genetics.* 2016;12:e1005939.
- 635 57. Petersen MH, Budtz-Jørgensen E, Sørensen SA, Nielsen JE, Hjermand LE, Vinther-Jensen T, et al.
636 Reduction in mitochondrial DNA copy number in peripheral leukocytes after onset of Huntington’s
637 disease. *Mitochondrion.* 2014;17:14–21.
- 638 58. Coskun PE, Wyrembak J, Derbereva O, Melkonian G, Doran E, Lott IT, et al. Systemic mitochondrial
639 dysfunction and the etiology of Alzheimer’s disease and down syndrome dementia. *J Alzheimers Dis.*
640 2010;20 Suppl 2:S293-310.
- 641 59. Park J-S, Davis RL, Sue CM. Mitochondrial Dysfunction in Parkinson’s Disease: New Mechanistic
642 Insights and Therapeutic Perspectives. *Curr Neurol Neurosci Rep [Internet].* 2018 [cited 2020 May
643 19];18. Available from: <https://www.ncbi.nlm.nih.gov/pmc/articles/PMC5882770/>
- 644 60. Wei W, Keogh MJ, Wilson I, Coxhead J, Ryan S, Rollinson S, et al. Mitochondrial DNA point mutations
645 and relative copy number in 1363 disease and control human brains. *Acta Neuropathol Commun*
646 [Internet]. 2017 [cited 2020 Jun 8];5. Available from:
647 <https://www.ncbi.nlm.nih.gov/pmc/articles/PMC5290662/>
- 648 61. Atkin G, Paulson H. Ubiquitin pathways in neurodegenerative disease. *Front Mol Neurosci [Internet].*
649 2014 [cited 2020 May 19];7. Available from: <https://www.ncbi.nlm.nih.gov/pmc/articles/PMC4085722/>
- 650 62. Rice AC, Keeney PM, Algarzae NK, Ladd AC, Thomas RR, Bennett JP. Mitochondrial DNA copy
651 numbers in pyramidal neurons are decreased and mitochondrial biogenesis transcriptome signaling is
652 disrupted in Alzheimer’s disease hippocampi. *J Alzheimers Dis.* 2014;40:319–30.
- 653 63. Delbarba A, Abate G, Prandelli C, Marziano M, Buizza L, Arce Varas N, et al. Mitochondrial Alterations
654 in Peripheral Mononuclear Blood Cells from Alzheimer’s Disease and Mild Cognitive Impairment
655 Patients. *Oxid Med Cell Longev.* 2016;2016:5923938.
- 656 64. Lv X, Zhou D, Ge B, Chen H, Du Y, Liu S, et al. Association of Folate Metabolites and Mitochondrial
657 Function in Peripheral Blood Cells in Alzheimer’s Disease: A Matched Case-Control Study. *J Alzheimers*
658 *Dis.* 2019;70:1133–42.
- 659 65. Lee J-W, Park KD, Im J-A, Kim MY, Lee D-C. Mitochondrial DNA copy number in peripheral blood is
660 associated with cognitive function in apparently healthy elderly women. *Clin Chim Acta.* 2010;411:592–
661 6.
- 662 66. Lee J-Y, Kim J-H, Lee D-C. Combined Impact of Telomere Length and Mitochondrial DNA Copy
663 Number on Cognitive Function in Community-Dwelling Very Old Adults. *DEM.* Karger Publishers;
664 2017;44:232–43.
- 665 67. Besnard A, Galan-Rodriguez B, Vanhoutte P, Caboche J. Elk-1 a Transcription Factor with Multiple
666 Facets in the Brain. *Front Neurosci [Internet].* 2011 [cited 2020 Jun 19];5. Available from:
667 <https://www.ncbi.nlm.nih.gov/pmc/articles/PMC3060702/>

- 668 68. Van Hout CV, Tachmazidou I, Backman JD, Hoffman JX, Ye B, Pandey AK, et al. Whole exome
669 sequencing and characterization of coding variation in 49,960 individuals in the UK Biobank [Internet].
670 Genomics; 2019 Mar. Available from: <http://biorxiv.org/lookup/doi/10.1101/572347>
- 671 69. Li H, Handsaker B, Wysoker A, Fennell T, Ruan J, Homer N, et al. The Sequence Alignment/Map
672 format and SAMtools. *Bioinformatics*. 2009;25:2078–9.
- 673 70. Robinson MD, Oshlack A. A scaling normalization method for differential expression analysis of RNA-
674 seq data. *Genome Biology*. 2010;11:R25.
- 675 71. Robinson MD, McCarthy DJ, Smyth GK. edgeR: a Bioconductor package for differential expression
676 analysis of digital gene expression data. *Bioinformatics*. 2010;26:139–40.
- 677 72. Kanehisa M, Goto S. KEGG: kyoto encyclopedia of genes and genomes. *Nucleic Acids Res*.
678 2000;28:27–30.
- 679 73. Balduzzi S, Rücker G, Schwarzer G. How to perform a meta-analysis with R: a practical tutorial. *Evid
680 Based Mental Health*. 2019;22:153–60.
- 681

Figure 1. Global inflation of test statistics from linear regressions between blood-derived mtDNA-CN and gene expression in blood. After stratification by gene category, protein-coding genes have the most inflation, suggesting that mtDNA-CN is strongly associated with genes that code for proteins.

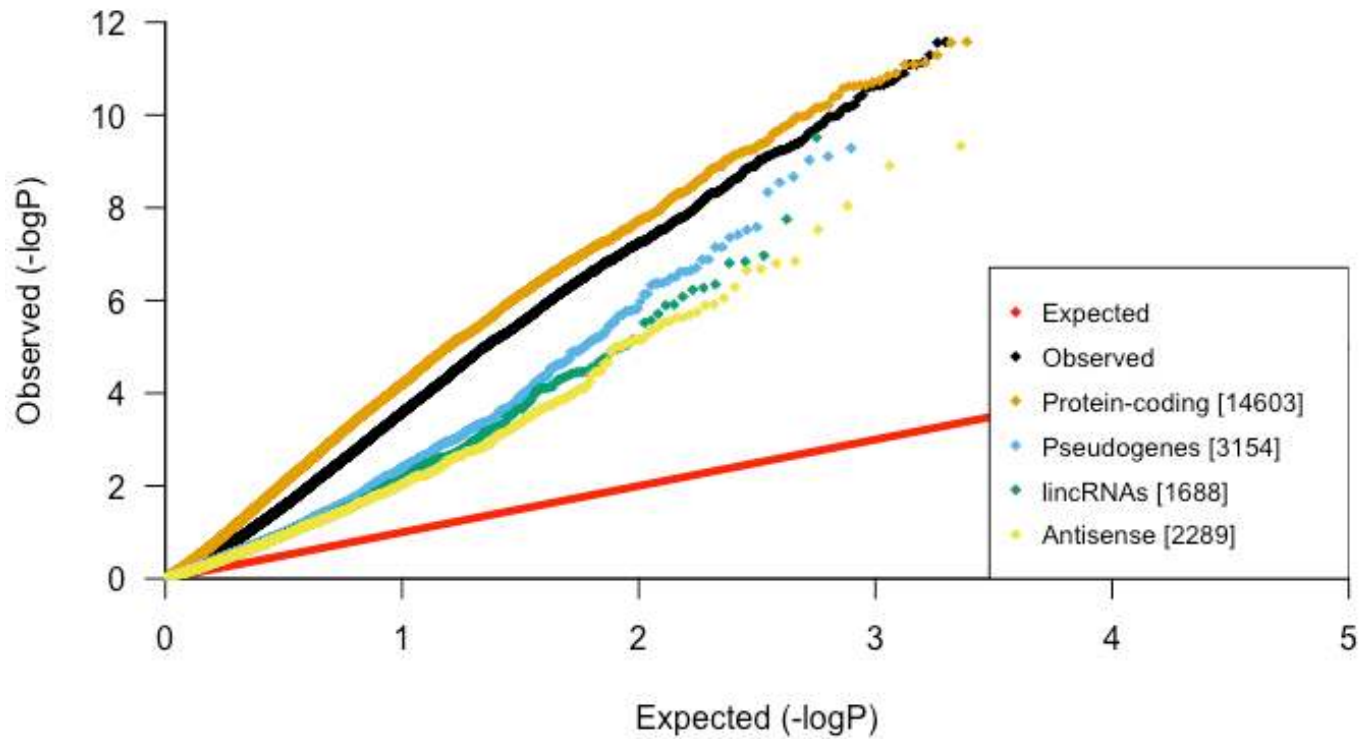


Figure 2. REVIGO visualization of GO Cellular Component terms significantly associated with mtDNA-CN after removal of redundant GO terms. Size of the circle represents the relative number of genes in each gene set, color represents significance. Axis represent semantic similarities between GO terms; GO terms that are more similar will cluster with one another.

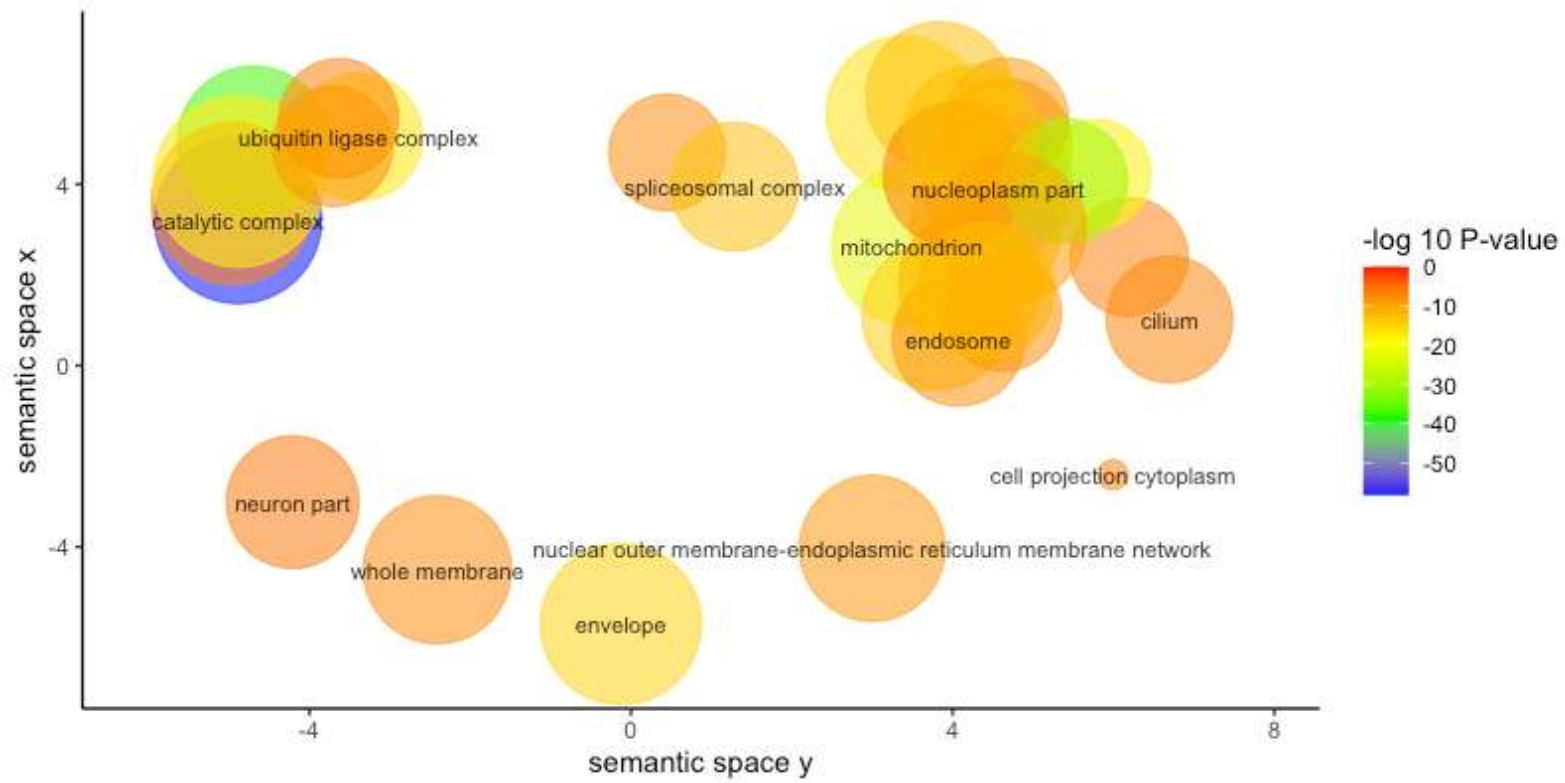


Figure 3. Observed genomic inflation factors are significantly different from permuted genomic inflation factors for certain tissues. Higher genomic inflation factor represents increased global associations between blood-derived mtDNA-CN and gene expression in a specific tissue. Permuted genomic inflation factors were obtained using two-stage permutation testing.

